ACADEMIC PRESS

Journal of Solid State Chemistry 169 (2002) 189–198

JOURNAL OF SOLID STATE CHEMISTRY

www.academicpress.com

Structures and magnetic properties of Ln_3OsO_7 (Ln = Pr, Nd, Sm)

J.R. Plaisier,[a,*] R.J. Drost,[b] and D.J.W. IJdo[a]

[a] *Leiden Institute of Chemistry, Gorlaeus Laboratories, Leiden University, P.O. Box 9502, 2300 RA Leiden, Netherlands*
[b] *Kamerlingh Onnes Laboratorium, Leiden University, P.O. Box 9506, 2300 RA Leiden, Netherlands*

Received 13 May 2002; received in revised form 18 September 2002; accepted 25 September 2002

Abstract

Polycrystalline samples of Ln_3OsO_7 (Ln = Pr, Nd, Sm) have been prepared. The structures of these compounds were determined by X-ray powder diffraction. They crystallize in a superstructure of cubic fluorite (space group *Cmcm*, $Z=4$). The samples have been characterized by magnetometry. The compounds show complex magnetic behavior at low temperatures caused by competing magnetic interactions leading to frustration.

Keywords: Osmium; Rare earth; Oxide; Linear chains; Structure; Magnetism

1. Introduction

Compounds of the general formula Ln_3MO_7 have attracted growing interest, because of their one-dimensional structural features and possible related magnetic properties. The parent structure of this family of compounds, La_3NbO_7, was first determined by Rossel [1]. The structure is an orthorhombic superstructure of the cubic fluorite type (lattice parameter a_c) with space group *Cmcm* and unit-cell parameters $a_{orth} \approx 2a_c$, $b_{orth} \approx c_{orth} \approx a_c\sqrt{2}$. The compounds contain infinite one-dimensional chains of corner-shared MO_6 octahedra. A large number of compounds containing platinum group metal ions at the M-site as well as related compounds have been characterized [2–5].

The one-dimensional chains of MO_6 octahedra may give rise to one-dimensional magnetic properties. Most rare earth metals, however, have a nonzero spin, which could lead to long-range order at some finite temperature due to Ln–M coupling. Recently, several papers have been published dealing with the magnetic properties of compounds containing Ru at the M-site [6–10].

In the context of a larger project dealing with the electrocatalytic properties of platinum group metal oxides, we have prepared compounds with Os^{5+} at the M-site. As has been shown earlier [11–13], a major problem in the preparation of osmium oxides is the formation of OsO_4, which is volatile. Furthermore, it is difficult to control the oxidation state of osmium, which in oxides ranges from 4+ to 8+. Synthesis of these compounds has to take place in a closed system, since the oxygen pressure in the experiments appears to play a very important role.

In the Ln–Os–O system only a few compounds have been reported. Shaplygin and Lazarev [14] reported the existence of the pyrochlore $Ln_2Os_2O_7$ (Os^{4+}). Furthermore, $Ln_4Os_6O_{19}$ was found for Ln = La and Nd [15,16]. These compounds have a structure related to that of $KSbO_3$ and Os is present in the formal oxidation state of 4.33. The only other ones in these systems known today are $La_3Os_2O_{10}$ [17] and $NdOsO_4$ [18]. In these systems, the latter compound is the only one reported containing pentavalent Os. In this paper the synthesis, structures and magnetic properties of Ln_3OsO_7 with Ln = Pr, Nd and Sm are presented.

2. Experimental

The samples were prepared from chemically pure grade Os and Ln_2O_3, Pr_6O_{11}, dried at 1000°C. The mixtures were heated in gold crucibles in a vacuum-sealed quartz tube. Ag_2O was added as oxygen donor in

*Corresponding author.
E-mail address: plaisier@chem.leidenuniv.nl (J.R. Plaisier).

0022-4596/02/$ - see front matter © 2002 Elsevier Science (USA). All rights reserved.
PII: S0022-4596(02)00057-9

a separate crucible. Since the pressure of oxygen plays a crucial role in the synthesis of ternary osmium oxides, various ratios of the starting compounds were heated at different temperatures. Most experiments yielded the pyrochlore $Ln_2Os_2O_7$ and Ln_2O_3. Nd_3OsO_7 was prepared by heating Nd_2O_3 and Os in the molar ratio 1:2 and an excess of Ag_2O at 500°C for 1 day in order to decompose Ag_2O. Next, the tube was heated at 750°C for 2 weeks, after which the quartz tube was opened. Finally, the gold tube was sealed and heated for 2 days at 950°C. This procedure yielded a mixture of Nd_3OsO_7 and a small amount of Nd_2O_3 which could be removed by washing with 0.1 M hydrochloric acid. Pr_3OsO_7 could be prepared in a similar way. In both cases Os was lost through the formation of OsO_4. Sm_3OsO_7 could be prepared by heating a stoichiometric mixture of Sm_2O_3 and Os and a stoichiometric amount of Ag_2O at 500°C for 1 day and at 750°C for 3 weeks. This procedure yielded a single phase. All products are black.

The reaction products were examined with a Philips PW 1050 X-ray diffractometer using monochromated Cu$K\alpha$ radiation. The data were collected digitally in steps of 0.02° 2θ and 14 s counting time in the range: $10^\circ \leqslant 2\theta \leqslant 90^\circ$. All data were collected at room temperature. Rietveld's method [19] was used to determine the structure. For this purpose the program FULLPROF [20] was used. A scale factor, six background parameters, the unit-cell parameters, the zero-point correction, the atomic fractional coordinates, one overall U_{iso}, five profile parameters defining the pseudo-Voigt shape of the reflections, and two asymmetry parameters were refined. As trial model the coordinates of Nd_3RuO_7 [5] were used.

Magnetic measurements were carried out in the temperature range 5–300 K by means of a Quantum Design MPMS-5S SQUID on approximately ~0.1 g of randomly oriented powder. Temperature sweeps were taken in both zero-field cooled (ZFC) mode and in field-cooled (FC) mode. The applied field was 0.1 T. Isothermal magnetization loops were recorded at 5, 10 and 15 K for Nd_3OsO_7 and at 5, 12 and 17 K for Sm_3OsO_7. AC susceptibility measurements were performed on both compounds in an applied field of 1 Oe with frequencies of 377 Hz for Nd_3OsO_7 and 3.7, 37 and 370 Hz for Sm_3OsO_7. The magnetic behavior of Pr_3OsO_7 was not studied, since the sample contained a small amount of a magnetic starting material.

3. Results

It proved possible to prepare Ln_3OsO_7 for $Ln = Pr$, Nd and Sm. The X-ray diffraction patterns of all samples except Sm_3OsO_7 clearly showed the presence of the target compounds as well as small amounts of the lanthanide oxides. Most compounds could be purified by washing the product with dilute hydrochloric acid and drying at 150°C. In the case of Pr_3OsO_7, however, Pr_6O_{11} could not be removed completely. Therefore, the latter compound was introduced as a second phase in the Rietveld refinement. Refinements of the structures of these compounds in the space group *Cmcm* were successful, leading to agreement factors: $12.8 \leqslant R_{wp} \leqslant 16.4$ and $1.44 \leqslant \chi^2 \leqslant 3.19$. The agreement between the observed and the calculated profiles of Nd_3OsO_7 is presented in Fig. 1. Table 1 shows the results of the Rietveld refinements.

The molar magnetic susceptibility of Nd_3OsO_7 in a field of 0.1 T is presented in Fig. 2. Clear divergences are apparent between the data measured under ZFC and FC conditions below ~75 K. Below this temperature, the FC susceptibility increases with decreasing temperature, and reaches a maximum at $T_{max} \approx 10$ K. Fig. 3 shows isothermal magnetization loops at 5, 10 and 15 K. At 15 K, which is just above T_{max} a large amount of hysteresis is observed. The center of this hysteresis loop is slightly displaced from the origin. With decreasing temperature the center of the loops moves further away from the origin. At the same time the amount of hysteresis decreases on cooling, almost completely disappearing at 5 K. AC susceptibility measurements performed in an applied field of 1 Oe with frequencies of 377 Hz are shown in Fig. 4. A large cusp in the in-phase susceptibility is observed at approximately 75 K. However, no transition is observed upon cooling further. In fact, the susceptibility appears to return gradually to paramagnetic behavior.

In Fig. 5 the molar susceptibility of Sm_3OsO_7 in a measuring field of 0.1 T is shown. The data presented show features similar to those observed for the Nd-analog. However, a few distinct differences are observed in the low-temperature region. The sharp increase in susceptibility occurs at a lower temperature of ~50 K, whereas the temperature of the maximum (T_{max}) in the FC susceptibility is somewhat higher (~20 K). Fig. 6 shows the region between 5 and 60 K for different magnetic fields. Isothermal magnetization loops at 5, 12 and 17 K are shown in Fig. 7. The loops are similar to those measured for Nd_3OsO_7. The amount of hysteresis decreases with decreasing temperature, whereas the displacement from the origin is increased. Fig. 7 shows the AC-susceptibility of Sm_3OsO_7 at different frequencies. The curves show only one transition close to 50 K. The transition temperature appears to be independent of the frequency used in the experiment.

The high-temperature regions of the susceptibility measurements were fitted against the Curie–Weiss law, which was extended to include a term for the temperature-dependent paramagnetic contribution (α). In the case of Nd_3OsO_7, the value found for the Weiss temperature was found to be zero within the error margin. This value was set to zero. This resulted in

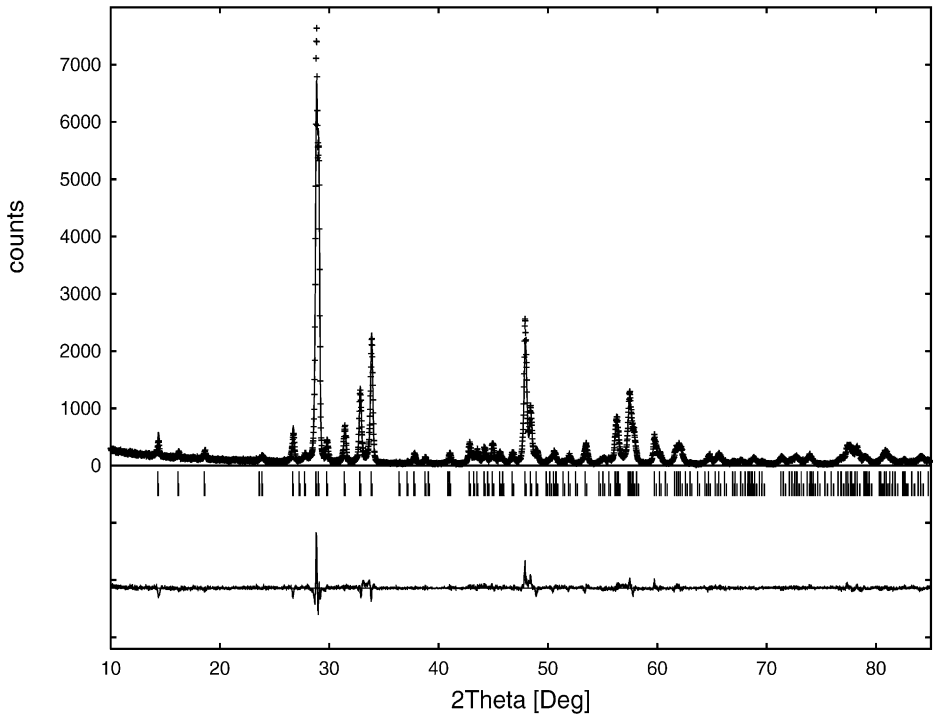

Fig. 1. Observed (crosses) and calculated (line) X-ray diffraction pattern of Nd_3OsO_7; the difference ($I_{obs} - I_{calc}$) curve at the bottom of the figure. Tick marks indicate the position of the Bragg reflections included in the calculation.

Table 1
Results of the Rietveld refinements for Ln_3OsO_7

		Pr_3OsO_7	Nd_3OsO_7	Sm_3OsO_7
a	(Å)	10.958(1)	10.8829(8)	10.707(2)
b	(Å)	7.457(1)	7.4303(6)	7.436(1)
c	(Å)	7.552(1)	7.5066(6)	7.473(1)
V	(Å^3)	617.1(1)	607.00(8)	594.8(2)
ρ	(g cm^{-3})	7.80(1)	8.04(1)	8.41(1)
$Ln(2)$	x	0.2273(2)	0.2260(2)	0.2305(2)
	y	0.3046(3)	0.3031(2)	0.2921(3)
O(1)	x	0.122(1)	0.131(1)	0.145(2)
	y	0.304(2)	0.306(1)	0.300(3)
	z	0.952(2)	0.955(2)	0.950(3)
O(2)	x	0.143(2)	0.133(2)	0.121(4)
	y	0.027(3)	0.021(2)	0.026(4)
O(3)	y	0.415(4)	0.422(3)	0.430(5)
U_{iso}	(Å^2)	0.0020(7)	−0.0057(5)	0.0083(7)
R_p		11.5	9.68	12.1
R_{wp}		14.9	12.8	15.8
χ^2		2.76	3.19	2.19
N_{var}		28	26	26

Note. $Ln(1)$ at 4a(0,0,0), $Ln(2)$ at 8g ($x, y, 1/4$), Os at 4b (0,1/2,0), O(1) at 16h (x, y, z), O(2) at 8g ($x, y, 1/4$), O(3) at 4c ($O, y, 1/4$).

proper fits (Nd_3OsO_7: $C = 3.49(2)$ emu K mol^{-1}, $\alpha = 5.4(1) \times 10^{-3}$; Sm_3OsO_7: $C = 0.291(6)$ emu K mol^{-1}, $\theta = -6.8(5)$ K and $\alpha = 3.09(6) \times 10^{-3}$. The results of these fits together with the expected Curie constants are given in Table 2. For comparison values for other Ln_3MO_7-type compounds obtained from the literature are included in the table.

4. Discussion

The results described above clearly indicate that Os^{5+} can be stabilized in an octahedral coordination sphere if enough care is exercised during preparation. Special attention for the preparation temperature and the oxygen pressure in the experiment is required. Slight differences in temperature resulted in the formation of the Os(IV) containing pyrochlore, which, once formed, proved impossible to remove by continued heating. Furthermore, an appropriate oxygen source must be chosen, since previous experiments with $KClO_3$ had shown that chlorine ions readily enter the lattice [11,12]. We found that Ag_2O is a very effective oxygen donor under our experimental conditions. Once the target compounds were formed, they appeared to be stable in air at temperatures up to 150°C and even in 0.1 N hydrochloric acid at room temperature. Since the ionic radius of Os^{5+} is similar to those of Ru^{5+} and Ir^{5+}, it was expected that preparing Eu_3OsO_7 would be possible too. However, attempts to synthesize this compound were unsuccessful.

A projection of this structure along the c-axis is given in Fig. 8. The MO_6 octahedra are corner-linked through

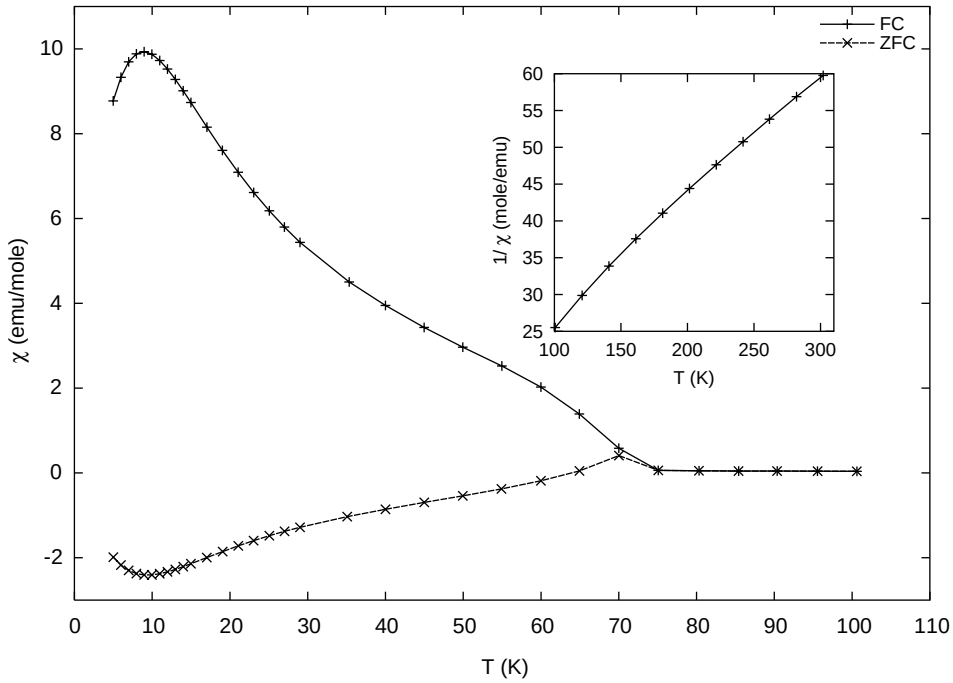

Fig. 2. Magnetic susceptibility as a function of temperature for Nd_3OsO_7.

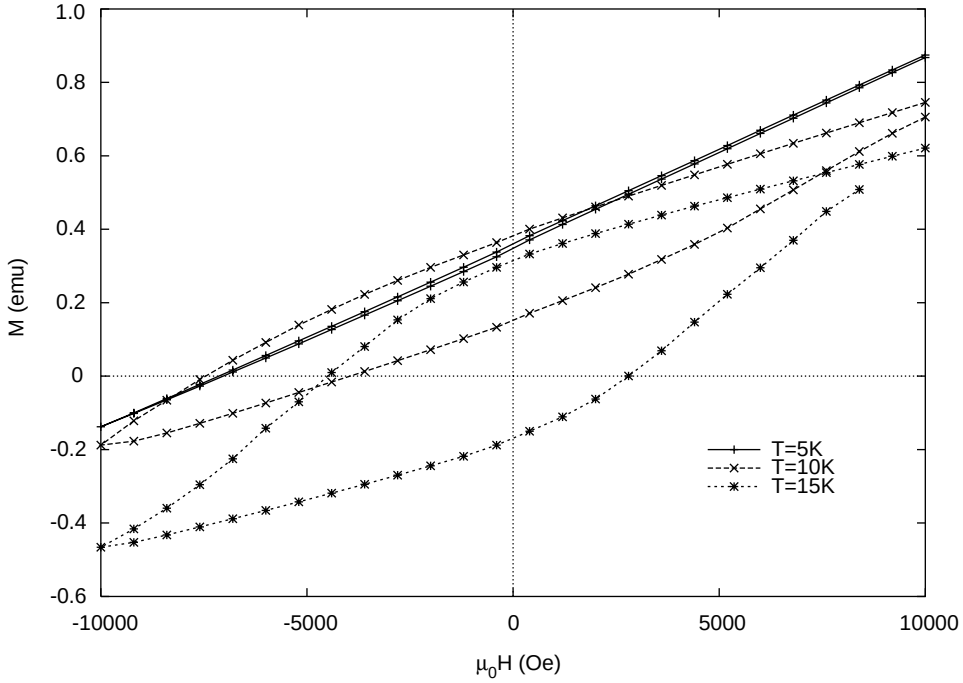

Fig. 3. Isothermal magnetization versus field at various temperatures for Nd_3OsO_7.

the O(3) atoms. Successive O(3) atoms lie in a row parallel to the *c*-axis in a zigzag sequence $(0, y, 1/4), (0, -y, 1/4), \ldots$, with $y \approx 0.4$, giving rise to a corresponding sequence of tilts to the octahedra. One-third of the] *Ln*-cations are in eight-fold oxygen coordination, lying in rows in the [001] direction, which alternate with the parallel zigzag chains of the corner sharing MO_6 octahedra, forming slabs parallel to the *b*–*c* plane. The remaining two-thirds are in seven coordination and lie between the slabs of the LnO_8 and the MO_6 polyhedra. Unfortunately, due to the difficulties encountered in the preparation of these

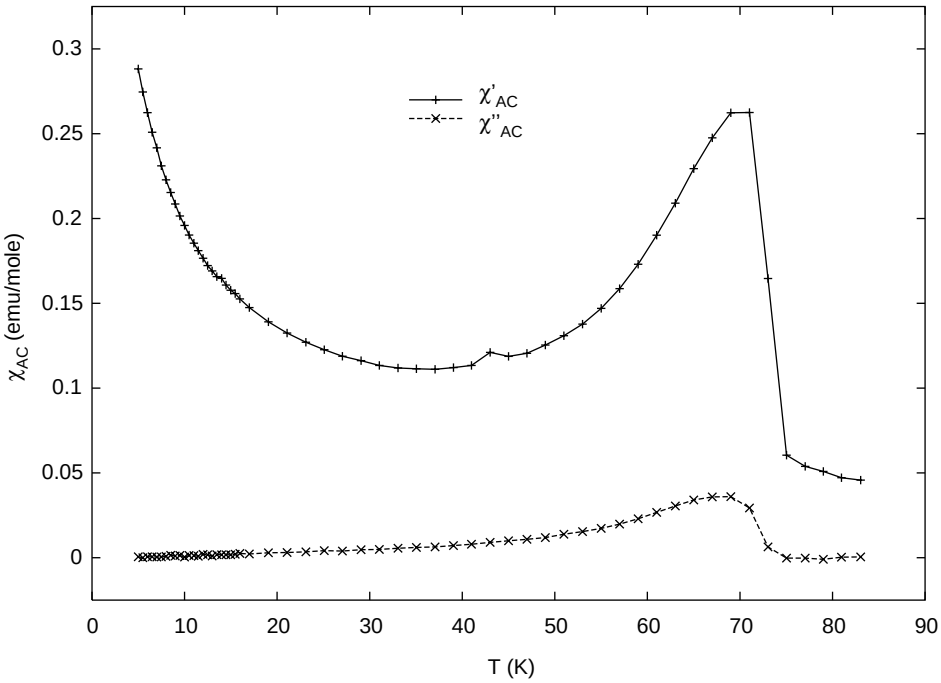

Fig. 4. AC magnetic susceptibility of Nd_3OsO_7 versus temperature.

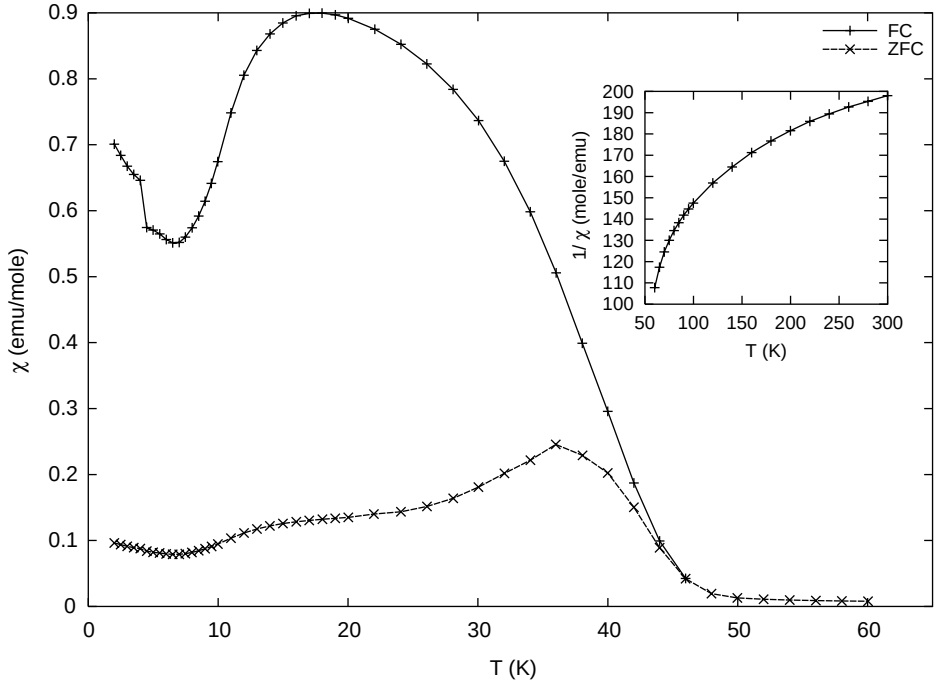

Fig. 5. Magnetic susceptibility as a function of temperature for Sm_3OsO_7.

compounds, we were unable to prepare amounts large enough to make a neutron diffraction experiment feasible, we have to rely on our structure determination based on X-ray powder data. As a result, a detailed discussion of the crystallographic data is impossible because of the large uncertainties in the atomic positions of the oxygen ions. However, we can draw some conclusions based on our cell parameters comparing them to those reported in the literature for isomorphous compounds. As can be seen in Table 3, the cell volumes of these Ln_3MO_7 compounds depend largely on the size of the lanthanide cation. The cell volumes differ by as

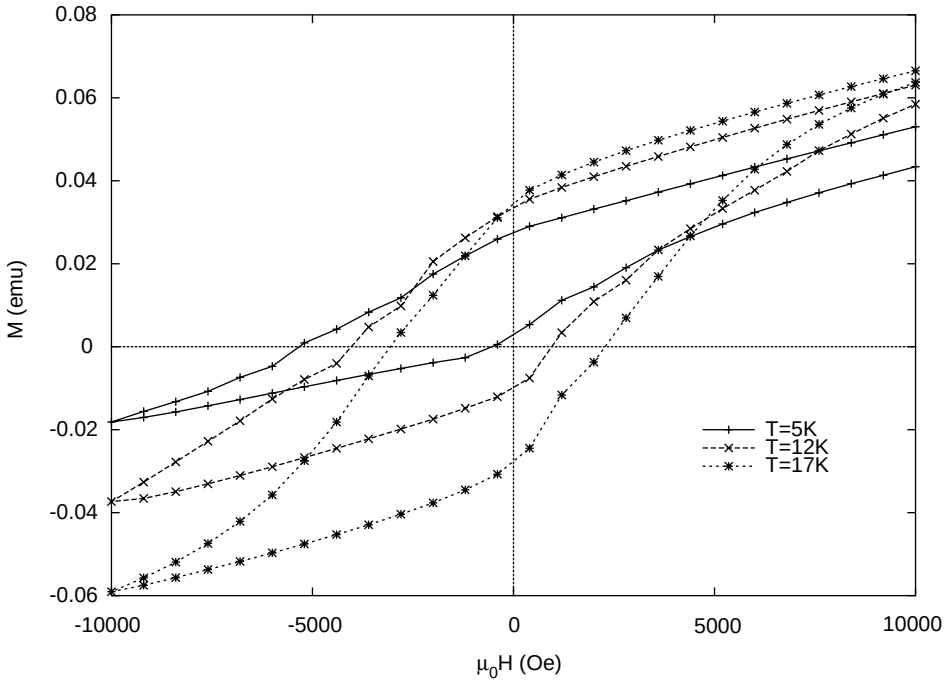

Fig. 6. Isothermal magnetization versus field at various temperatures for Sm_3OsO_7.

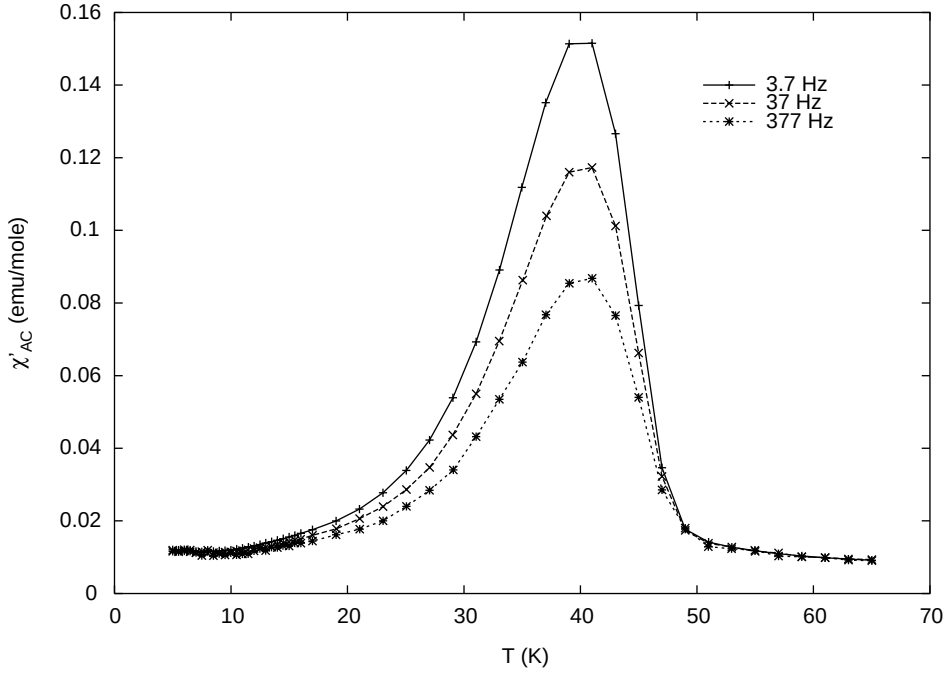

Fig. 7. AC magnetic susceptibility of Sm_3OsO_7 versus temperature.

much as 12%. Surprisingly, however, the ratio between the intra-chain M–M distance and the inter-chain M–M distance is virtually independent of the composition. This feature is observed too in a series of compounds with the same M-cation. For Ln_3RuO_7, for which most data are available, the volume differs by around 9%, whereas the intra-chain to inter-chain ratio only differs by approximately 1%. This indicates that the expansion is highly isotropic, despite the fact that the structure appears to be one-dimensional. The shortening of the c-axis is likely to be accommodated by an increased buckling of the M–O(3)–M angle ($\sim 150^\circ$) within the

Table 2
Magnetic constants of Ln_3MO_7 compounds

Compound	Fit-region (K)	C (emu K mol^{-1})	C_{exp} (emu K mol^{-1})	θ (K)	Reference
La_3RuO_7	50–300	1.958	1.87	−14	[6]
Pr_3NbO_7	80–300	3.14(2)	4.58	−18.0(6)	[3]
Pr_3RuO_7	200–350	5.90	6.69	2.2	[10]
Pr_3SbO_7	25–300	3.12(2)	4.58	−24(4)	[3]
Pr_3TaO_7	80–300	3.18(4)	4.58	−19(1)	[3]
Pr_3IrO_7	80–300	3.09(2)	4.58	−7.1(8)	[27]
Nd_3IrO_7	80–300	2.97	4.58	−6.8(5)	[27]
Nd_3RuO_7	100–300	6.54	6.69	−26	[9]
Nd_3OsO_7	85–300	3.49(2)	5.93	∼0	—
Sm_3ReO_7	4–52	0.045(1)	0.84	−1.4(1)	[26]
Sm_3OsO_7	70–300	0.291(6)	2.19	−8(1)	—

chain. However, our data, as well as most of the reported values of this angle, are not precise enough to draw any firm conclusions.

Now we turn to the magnetic properties. In the high-temperature regions both osmium oxides investigated appear to follow the Curie law for paramagnetic solids. However, the Curie constants derived from these measurements have unexpectedly low values. Examination of these values in other compounds with the formula Ln_3MO_7 (Table 2) shows that this is the case for all compounds except Ln_3RuO_7. In order to explain this observation one must first look at the compounds Pr_3MO_7 with M = Nb, Sb and Ta and Ln_3IrO_7 with Ln = Pr and Nd. The first group contains a non-magnetic cation at the B-site, whereas the latter contains Ir^{5+} at this site, which has an effective magnetic moment which is proportional to the square root of the temperature [21]. As a result, the contribution of the M-cations to the Curie constants for all these compounds is expected to be zero. The expected contribution from the neodymium and praseodymium cations is comparable. The differences between the reported values are indeed very small. From these values the effective magnetic moment per rare earth cation is calculated to be $\sim 2.9\ \mu_B$. This is considerably smaller than the expected moment of $3.6\ \mu_B$. Apparently, the crystal-field effects on these cations are rather large, leading to a reduction of the magnetic moments of the same order of magnitude. Only two Ln_3MO_7-type compounds have been reported where the M-cation is the only ion with a magnetic moment. La_3RuO_7 contains ruthenium in a $4d^3$ configuration ($S = \frac{3}{2}$). The reported value for the Curie constant indicates classical spin behavior with an effective moment close to the spin-only value for Ru^{5+}. La_3MoO_7 shows no paramagnetic behavior up to 800 K [22]. Little is known about the magnetic properties of pentavalent osmium in oxides. The magnetic properties of only three Os^{5+} oxides with the pyrochlore structure have been reported

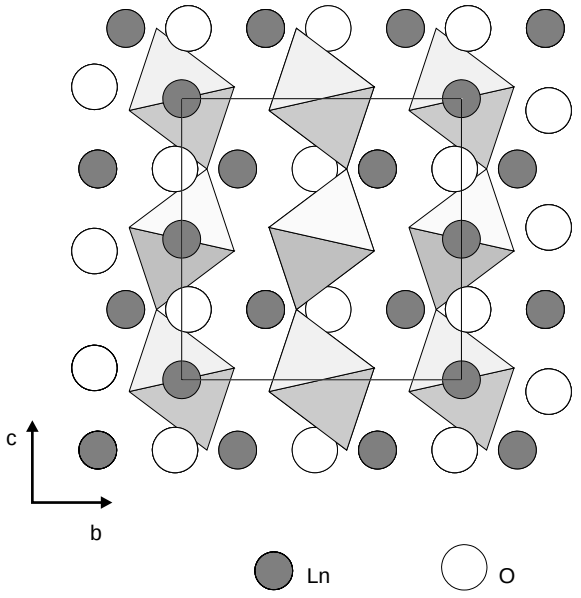

Fig. 8. Projection of the structure of Ln_3MO_7 along the a-axis.

[23]. All three compounds show Pauli-paramagnetic behavior. However, effective moments ranging between 3 and 3.3 μ_B have been found in fluorides and chlorides [24,25]. Using the values obtained from the compounds with a non-magnetic B-ion, it is possible to calculate the contribution of Os^{5+} ($5d^3$) to the Curie constant of Nd_3OsO_7. Assuming an effective moment of 2.9 μ_B per Nd^{3+} the effective moment of Os^{5+} is found to be $\sim 1.93\ \mu_B$. Since for $5d^3$ ions spin–orbit coupling cannot be ignored, the expected moment of Os^{5+} is lower than the spin-only value of 3.87 μ_B. Therefore, in the absence of experimental data on the moments of Os^{5+} in oxides, the expected value is taken from the chlorides and fluorides mentioned ($\sim 3.3\ \mu_B$). The value found here is clearly lower. It is difficult to use a similar method in order to find the contribution of Os^{5+} to the Curie constant of Sm_3OsO_7. The only other reported

Table 3
Structural parameters of Ln_3MO_7-type compounds

	a (Å)	b (Å)	c (Å)	V (Å^3)	V_{rel}	r_{intra}/r_{inter}	Reference
Pr_3OsO_7	10.958(1)	7.457(2)	7.552(1)	617.1(1)	0.934	0.570	—
Nd_3OsO_7	10.8823(8)	7.4303(6)	7.5066(6)	606.97(8)	0.919	0.570	—
Sm_3OsO_7	10.707(2)	7.436(1)	7.473(1)	594.8(2)	0.901	0.573	—
La_3RuO_7	11.2093(1)	7.4617(1)	7.6077(8)	636.31(2)	0.963	0.565	[6]
Pr_3RuO_7	10.9806(2)	7.3841(1)	7.5311(1)	610.63(2)	0.924	0.569	[10]
Nd_3RuO_7	10.9043(5)	7.3811(3)	7.4955(3)	603.29(4)	0.913	0.569	[9]
Sm_3RuO_7	10.7552(2)	7.3356(1)	7.4375(1)	586.79(2)	0.888	0.571	[8]
Eu_3RuO_7	10.6927(1)	7.3228(1)	7.4125(1)	580.40(1)	0.879	0.572	[8]
La_3NbO_7	11.167(1)	7.629(1)	7.753(1)	660.5(1)	1.000	0.573	[1]
Pr_3NbO_7	10.959(1)	7.5240(7)	7.6676(7)	632.3(1)	0.957	0.577	[3]
Nd_3NbO_7	10.905(2)	7.517(2)	7.624(1)	625.0(2)	0.946	0.576	[1]
La_3MoO_7[a]	11.0953(8)	7.597(1)	7.7192(4)	650.7(1)	0.985	0.574	[22]
Nd_3MoO_7	10.804(5)	7.505(2)	7.60(2)3	616.5(3)	0.933	0.578	[29]
La_3SbO_7	11.1509(7)	7.6299(5)	7.7424(5)	658.73(9)	0.997	0.573	[30]
Pr_3SbO_7	10.9442(6)	7.5589(4)	7.6639(4)	634.01(8)	0.960	0.576	[3]
La_3TaO_7	11.173(2)	7.619(1)	7.755(1)	660.2(1)	0.999	0.573	[30]
Pr_3TaO_7	10.973(1)	7.5230(7)	7.6721(7)	633.9(1)	0.959	0.577	[3]
Sm_3ReO_7	10.736(5)	7.392(3)	7.519(3)	596.7(5)	0.903	0.576	[26]
Pr_3IrO_7	10.9795(3)	7.4379(2)	7.5374(2)	615.55(4)	0.932	0.568	[2]
Nd_3IrO_7	10.8903(7)	7.4400(5)	7.4893(5)	606.82(9)	0.919	0.568	[2]
Sm_3IrO_7	10.7375(5)	7.4028(4)	7.4336(4)	590.88(3)	0.895	0.570	[2]
Eu_3IrO_7	10.6746(8)	7.3871(7)	7.4087(6)	584.21(9)	0.884	0.571	[2]

[a] Space group $P2_12_12_1$.

compound with Sm^{3+} ions is Sm_3ReO_7 [26]. The reported Curie constant for this compound is very low, and the authors assume that the temperature dependence of the magnetization of this compound is only due to the rhenium ions. Using the same assumption in the case of Sm_3OsO_7 gives an effective moment of 1.52 μ_B per Os^{5+}. However, neither can the magnetic moment of Sm^{3+} be neglected, nor does it follow the Curie law. Therefore, based on the measurements presented in this paper, no firm conclusions can be drawn on the effective moments of both cations in this compound. Clearly, the contribution of the Os cations is lower than expected in both cases. The difference with the expected values is too significant to neglect. There are several possible explanations for this reduction. Nd_3IrO_7 is reported to be a good electrical conductor at temperatures below 800 K [27]. The conductivity is explained by the formation of an Ir–O–Ir conduction band along the chains. This delocalization of electrons of the M-ions may lead to a reduced magnetic moment. The M–O–M angles in the chains deviate from 180° leading to a decreased overlap between the d_M and p_O orbitals and a consequent decrease in electronic bandwidth. In ruthenium-based pyrochlores, an angle of 133° is thought to be the minimum angle enabling metallic behavior [28]. In pyrochlores, however, the octahedra form a three-dimensional network, which is less vulnerable to defect scattering than the chains found in these compounds. For this reason Khalifah et al. [6] conclude that La_3RuO_7 is semi-conducting along the chains. Another explanation may be the presence of short-range magnetic correlation in the chains as was found for La_3MoO_7 [22]. In order to find evidence for this the magnetic susceptibility should be measured up to much higher temperatures. However, due to the low thermal stability of compounds containing osmium, this method is not applicable in our case.

At low temperatures both compounds show a complex behavior. A sharp rise in the DC-susceptibilities is found at $T = 75$ K (Ln = Nd) and 48 K (Ln = Sm). At the same temperature the ZFC and FC measurements start to diverge, which is indicative of a spin-glass-like state below these temperatures. The negative value of the ZFC susceptibility of Nd_3OsO_7 is probably the effect of a small remanent magnetic field in the measurement apparatus. The broad maxima at lower temperatures (T_{max}) are indicative of antiferromagnetic interactions. Interestingly, this maximum is also observed as a minimum in the negative values of the ZFC susceptibility of Nd_3OsO_7. The results obtained here should be compared to those published for the ruthenium analogues. For Ln = La and Pr, Ln_3RuO_7

shows antiferromagnetic properties at low temperatures [6,8–10]. For $Ln = Nd$, Sm and Eu [8,9] weak antiferromagnetic transitions are found at approximately 20 K. A resulting weak ferromagnetic moment gives rise to a sharp increase of the susceptibility below T_N. This transition is attributed to coupling of Ru^{5+} spins. A similar explanation could be given here in order to explain the increase of the susceptibility of the compounds discussed in this paper. Only for Nd_3RuO_7 a maximum in the magnetic susceptibility is observed below T_N, which, according to the authors, is caused by the Nd^{3+} ions. The magnetic susceptibility of this compound is similar to those presented here. Neutron diffraction experiments indicated antiferromagnetic ordering of the ruthenium spins parallel to the *b*-axis.

In order to examine the different transitions, we should turn to the AC-susceptibility measurements and the magnetization loops. The in-phase AC susceptibility of both Ln_3OsO_7 compounds show a sharp increase around T_N. This increase is accompanied by an increase of the out-of-phase component of the susceptibility. This latter feature is an indication of long relaxation times. However, for both compounds no transition is found at temperatures below T_N. Instead, a gradual decrease of the susceptibility is observed in the case of Nd_3OsO_7, returning to paramagnetic behavior again at low temperatures. The temperature of the maximum AC susceptibility of Sm_3OsO_7 appears to be independent of the frequency (Fig. 7). In the case of spin-glass-like magnetism usually a shift to lower temperatures is found with increasing frequencies. Apparently, the transition at T_N is not a transition to a spin-glass state. This observation is confirmed by the magnetization loops shown in Figs. 3 and 6. The loops show a large amount of hysteresis, indicative of slow relaxation. However, below T_{max} the center of the loops starts shifting away from the origin. This shift, which is caused by freezing of the spins, illustrates the presence of a spin-glass-like state below T_{max}. This state could be caused by the coupling of the *Ln*-spins, leading to competitive interactions. On cooling below T_{max}, the hysteresis in the M–H curves gradually decreases and for Nd_3OsO_7 it has almost completely disappeared at 5 K. Apparently, the moment of the frustrated sublattice is completely frozen at this temperature, leading to a permanent moment and paramagnetic contribution of the other sublattice.

The low-temperature behavior of these compounds is clearly quite complex. The M–H curves also show no saturation below 1 T, making it difficult to determine which spins are involved in the different coupling. In the case of the ruthenium analogues [8–10] structural transitions are reported as well. These transitions have no effect on the magnetic properties of these compounds. In our investigations, we have seen no evidence for any structural transition. Based on the behavior of the ruthenium analogues and the transition temperatures of the compounds presented here, we assume that the magnetic transitions are not related to crystallographic transitions. Apparently, the behavior should be interpreted in terms of a magnetic structure composed of different sublattices, which leads to frustration.

5. Conclusions

The compounds Ln_3OsO_7 for $Ln = Pr$, Nd and Sm have been prepared for the first time. The formation of these Os^{5+} compounds appears to be extremely dependent on the oxygen pressure. The compounds were found to crystallize in the space group *Cmcm*. Examination of the structural features of these and the earlier reported Ln_3MO_7-type compounds leads to the conclusion that the structural behavior does not show one-dimensionality as would be expected.

The magnetic properties of Nd_3OsO_7 and Sm_3OsO_7 have been investigated. Both compounds show two transitions at low temperatures. The first transition is a weak ferromagnetic transition, which is caused by a coupling of the osmium spins. At lower temperatures the susceptibilities reach a maximum and decrease below this temperature. The second transition is probably caused by the Ln^{3+} ions. The magnetic behavior is similar to that of Nd_3OsO_7. Below T_{max} a spin-glass-like state is observed. The nature of this freezing is difficult to pin down, but is most likely caused by competing interactions of the different sublattices.

References

[1] H.J. Rossel, J. Solid State Chem. 27 (1979) 115.
[2] J.F. Vente, D.J.W. IJdo, Mater. Res. Bull. 26 (1991) 1255.
[3] J.F. Vente, R.B. Helmholdt, D.J.W. IJdo, J. Solid State Chem. 108 (1994) 18.
[4] F.P.F. van Berkel, D.J.W. IJdo, Mater. Res. Bull. 21 (1986) 1103.
[5] W.A. Groen, F.P.F. van Berkel, D.J.W. IJdo, Acta Crystallogr. C 43 (1987) 2262.
[6] P. Khalifah, R.W. Erwin, J.W. Lynn, Q. Huang, B. Batlogg, R.J. Cava, Phys. Rev. B 60 (1999) 9573.
[7] F. Wiss, N.P. Raju, A.S. Wills, J.E. Greedan, Int. J. Inorg. Mater. 2 (2000) 53.
[8] D. Harada, Y. Hinatsu, J. Solid State Chem. 158 (2001) 245.
[9] D. Harada, Y. Hinatsu, Y. Ishii, J. Phys.: Condens. Matter 13 (2001) 10 825.
[10] D. Harada, Y. Hinatsu, J. Solid State Chem. 164 (2002) 163.
[11] J.R. Plaisier, R.A.G. de Graaff, D.J.W. IJdo, Mater. Res. Bull. 30 (1995) 1249.
[12] J.R. Plaisier, R.A.G. de Graaff, D.J.W. IJdo, Mater. Res. Bull. 31 (1996) 279.
[13] J.R. Plaisier, D.J.W. IJdo, Mater. Res. Bull. 36 (2001) 1117.
[14] I.S. Shaplygin, V.B. Lazarev, Mater. Res. Bull. 8 (1973) 761.
[15] F. Abraham, J. Trehoux, D. Thomas, Mater. Res. Bull. 12 (1977) 43.
[16] F. Abraham, J. Trehoux, D. Thomas, J. Less Common Met. 77 (1981) 23.

[17] F. Abraham, J. Trehoux, D. Thomas, J. Solid State Chem. 29 (1979) 73.
[18] F. Abraham, J. Trehoux, D. Thomas, J. Inorg. Nucl. Chem. 42 (1980) 1627.
[19] H.M. Rietveld, J. Appl. Cryst. 2 (1969) 65.
[20] J. Rodriguez-Carvajal, FULLPROF Version 3.5, LLB-JRC, Saclay, France, 1997.
[21] Hayashi, G. Demazeau, M. Pouchard, P. Hagenmuller, Mater. Res. Bull. 15 (1980) 461.
[22] J.E. Greedan, N.P. Raju, A. Wegner, P. Gougeon, J. Padiou, J. Solid State Chem. 27 (1979) 115.
[23] B.L. Chamberland, Mater. Res. Bull. 13 (1978) 1273.
[24] T. Betz, R. Hoppe, Z. Anorg. Allg. Chem. 524 (1985) 17.
[25] Earnshaw, B.N. Figgis, J. Lewis, R.D. Peacock, J. Chem. Soc. (1961) 3132.
[26] G. Wltschek, H. Paulus, I. Svoboda, H. Ehrenberg, H. Fuess, J. Solid State Chem. 125 (1996) 1.
[27] J.F. Vente, Iridium Oxide Compounds, Ph.D. Thesis, Leiden University, 1994.
[28] K.-S. Lee, D.-K. Seo, M.-H. Whangbo, J. Solid State Chem. 131 (1997) 405.
[29] H. Czeskleba-Kerner, B. Cros, B. Tourne, J. Solid State Chem. 37 (1981) 294.
[30] J.G. Allpress, H.J. Rossell, J. Solid State Chem. 27 (1979) 105.